

超灵敏检测中信号扰动分析及应用

胡玉林¹, 华宇², 刘扬², 吴增强^{2*}

¹南通大学化学化工学院, 江苏 南通

²南通大学公共卫生学院, 江苏 南通

收稿日期: 2022年4月24日; 录用日期: 2022年5月9日; 发布日期: 2022年5月18日

摘要

随着相关技术的发展, 分析检测方法正在逐步向亚皮摩尔的检测限逼近的同时也面临一系列挑战。其中最大的挑战是目标分子或离子检测浓度的降低使相应的检测信号也降低, 甚至有可能低于环境的背景噪音, 以致于实际的检测信号被掩盖。为解决这一问题, 关键在于提高检测技术的信噪比。因此, 这篇综述主要探讨了超灵敏检测的进展和面临的挑战以及如何提高信噪比的方法。其中包括利用纳米孔和纳米通道的限域效应来放大目标检测物的信号的方法, 但是仍然存在如何降低背景噪音的问题, 因为限域的空间对信号放大是没有选择性的。另一种思路是利用噪音扰动分析, 对检测信号进行时域或频域的相关处理, 将其从背景噪音中分离, 从而获得检测物的具体信息。最后, 本综述结合这两个方面解决思路对超灵敏检测的未来发展作出了展望。

关键词

超灵敏检测, 信号扰动, 噪音分析, 纳米限域效应, 时域信号, 频域信号

Analysis and Application of Signal Fluctuation in Ultra-Sensitive Detection

Yulin Hu¹, Yu Hua², Yang Liu², Zengqiang Wu^{2*}

¹School of Chemistry and Chemical Engineering, Nantong University, Nantong Jiangsu

²School of Public Health, Nantong University, Nantong Jiangsu

Received: Apr. 24th, 2022; accepted: May 9th, 2022; published: May 18th, 2022

Abstract

The ultra-sensitive determination methods have been approaching to Sub-Picomolar detection

*通讯作者。

limit as well as confronting a series of challenges, where the greatest challenge we have to overcome is that lower level of detected signal resulting from lower concentration of target molecules is normally masked by background noise. Improving signal to noise ratio (S/N ratio) of detection method is a critical solution to address this concern. Therefore, in this review, we summarized the recent advances and challenges in ultra-sensitive detection and discussed methods to improve S/N ratio. Applying nano-confined effect of nanopore and nanochannel to amplify detected signal of target molecules is an efficient strategy. Meanwhile, since background noise is also magnified, reducing background noise is still a limiting factor in developing ultra-sensitive detection. Another strategy is to separate detected signals that are masked by background signal by applying noise analysis with the help of numerical method. Finally, we provide a brief discussion about future trend in developing ultra-sensitive detection.

Keywords

Ultra-Sensitive Detection, Signal Fluctuation, Noise Analysis, Nano-Confined Effect, Time Domain Signal, Frequency Domain Signal

Copyright © 2022 by author(s) and Hans Publishers Inc.

This work is licensed under the Creative Commons Attribution International License (CC BY 4.0).

<http://creativecommons.org/licenses/by/4.0/>



Open Access

1. 引言

随着分析检测技术的发展,生物传感器已经在疾病和健康监测等方面取得了很大的成功。比如,在血糖、孕检等方面已实现了快速、即时检测[1],也即是实现了床边检测(point of care, POC)的目标。然而,要实现生物传感器更广泛的应用,能否实现对更低浓度的被分析物的检测是其关键。例如,体液中的疾病标志物以及血液中的蛋白标志物的浓度范围都在 10^{-12} mol/L 到 10^{-9} mol/L 之间[2],而其中的病毒、肿瘤细胞的循环核酸、血液感染等的浓度范围低于 10^{-12} mol/L [3]。为达到这一目标,必须提高检测方法和仪器的灵敏度和检测限。目前,通过降低背景噪音、在线富集、提高信噪比等方法,已经实现了部分疾病标志物的检测。但对亚皮摩尔级别(浓度低于 10^{-12} mol/L)标志物的检测仍然是一项艰巨的挑战。这不仅是因为标志物分子的总数在降低,而且生理原因导致了难以利用现有采样方法来提高标志物分子的浓度(例如,血脑屏障限制了疾病标志物进入血液中的浓度)。随着检测物浓度的降低和检测体积的减小,要保持较高的检测灵敏度和检测限,需要检测方法逐渐逼近单分子检测的程度。相比于传统的基于系综水平的检测信号,超灵敏以及单分子检测中环境噪音和被检测分子的自身的随机扰动对检测信号的影响较大。而在信号处理方法得到广泛应用之前,这些单个分子或粒子自身行为造成的扰动通常会被掩盖在环境噪音信号中。因此,为实现对极低浓度疾病标志物的检测,必须对这些扰动产生的原因和揭示扰动自身所要传达的信息进行分析。

由于实验中记录的数据为检测信号与时间的关系,也就是时域的信号。从时域信号的分布来看,检测信号的扰动都是以信号的平均值为基准上下浮动,而检测信号值偏离平均值的范围在一定程度上反映了被检测物在稳态条件下的平衡信息(例如,结合常数等)。而从频域的角度来分析信号扰动的频率,再结合傅里叶变换可以获得被检测物的动力学特性[4]。另外,信号的扰动也反映了分子的构象变化以及分子之间相互作用等信息。但是,如何从这些扰动信号中获得相关信息,仍然是一项艰巨的挑战。要解决这一难题,则需要实验设计,数据分析等方面的交叉融合。本文主要从力学、电化学和光学检测三个方面概述利用检测信号的变化获取特定生物分子信息的方法及其发展趋势。

2. 基于力学动态响应的检测

基于原子力显微镜(atomic force microscope, AFM)悬臂的微小位移的检测技术,在激光的辅助作用下能够测量出皮牛级别(10^{-12} N)的力对悬臂引起的偏移。该技术被应用于生物分子相互作用[5] [6] [7] [8],微生物及细胞[9] [10] [11] [12]以及酶等生物分子吸附过程检测,并且发展到单个细胞和生物分子的检测中[13] [14] [15]。为获取单个生物分子间的识别过程, Bizzarri 等[5]采用动态力学谱技术从单分子层面研究了生物素-亲和素复合物的解离过程,测量了该解离过程的力学扰动,将该扰动与解离过程中分子结合势能变化联系起来,通过功率谱密度分析将力学扰动信号 $1/f$ 噪音与复合物形成过程关联起来。此外,该课题组[8]还研究了球蛋白分子间相互作用,揭示了球蛋白分子间相互作用的距离,通过噪音谱分析结果表明蛋白质的水化层动态扰动也展现出 $1/f$ 噪音的现象,据此推断水化层分子的变化对生物分子间识别过程的调节具有重要作用。由于细菌等微生物在代谢过程中,自身的运动会发生相应的变化。因此,可以利用 AFM 的悬臂来监控细菌在不同环境刺激(如抗生素、营养源)下扰动幅度的变化,并且绘制出不同细菌的抗菌图谱[10],如图 1 所示。这种基于纳米力学的振荡检测器能够为生物分析提供足够的时间精度,并且能揭示传统分析方法不能发现的微生物代谢或酶催化过程中的一些细节(例如,细菌的鞭毛抑制效应[16],蛋白构象变化[17]等)。相对于其他微纳米尺度表征技术而言,该技术对样品的损伤较小,可以适应不同环境的样品检测,因而其能够成为一个多功能的检测技术用于细胞和亚细胞尺度中多种生物物理参数测量[18]。另外,基于 AFM 的力学扰动检测还可以与激光共聚焦显微镜(LSCM)、全内反射荧光显微镜(TIRFM)、随机光学重构显微镜(STORM)等结合在更高的空间分辨(纳米)和时间分辨(毫秒)尺度上研究细胞和生物分子的生物物理性质。例如,Newton 课题组将激光共聚焦显微镜与 AFM 的悬臂检测结合,研究病毒在哺乳动物细胞表面的结合过程[19]。从目前的趋势来看,基于 AFM 悬臂的力学检测在单个细胞和生物分子检测上仍然有很大发展,重点在于提高检测的分辨率。

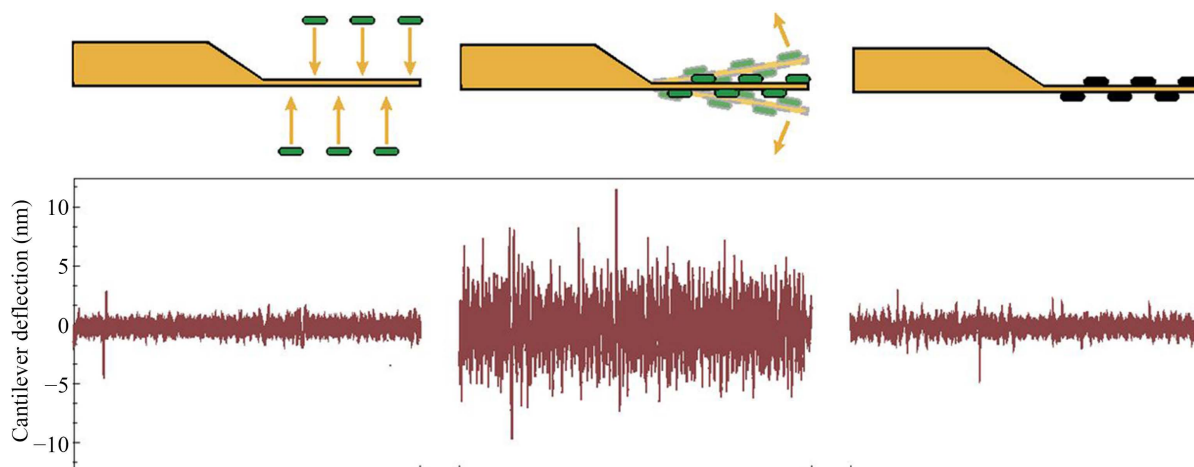


Figure 1. Detailed depiction of a nanomotion detection experiment. Before the attachment of the living specimens to the sensor, the fluctuations are small (Left). When the specimens are immobilized on the sensor, its fluctuations increase (Center). Finally, if the microorganisms are killed, through a chemical or physical agent, the sensor reverts to small fluctuations (Right). Reprinted with permission from ref. [10]. Copyright 2015 American Academy of Sciences

图 1. 纳米尺度移动检测实验示意图[10]。在活的样本吸附在传感器之前,扰动很小(左图)。当样本被固定在传感器上时,扰动增加(中间图)。最终,当微生物被化学或物理手段处理之后,传感器恢复之前的小扰动状态

3. 基于电化学信号扰动的分析

电化学检测方法具有响应灵敏度高、简便、易于操作的特点,在生化传感方面有着极其广泛的应用。

然而，电化学传感器的灵敏度和检测限容易受到环境及样品中其它物质的影响。传统的解决方法是抑制噪音和采用富集方式提高检测物浓度的方式来增大检测信号；通过检测信号的扰动来对检测物质的信息进行分析的方法则是另一种解决方案。通过对信号扰动源进行分析拆解，将本征的仪器噪音扰动与热扰动和检测物自身的扰动分解，再利用数学方法对扰动信号分析获取所需的信息。这种方法可以极为有效地提高电化学检测方法的精密度和灵敏度。

3.1. 电化学阻抗谱

电化学阻抗谱是通过在电极的直流电压上施加一定的交流电压的扰动，从而获得电极电流与响应频率之间的关系。Roy Chaudhuri 在纳孔二氧化硅基底上通过抗原抗体相互作用，利用电化学阻抗峰频率的变化实现了对食品中黄曲霉毒素 B1 的检测，检测限达到 1 fg/mL [20]。当黄曲霉毒素 B1 的浓度降低到亚飞摩尔时，电化学信号受到检测界面离子随机运动，抗原抗体结合过程扰动和检测装置本身扰动影响较大，很难直接观察到黄曲霉毒素 B1 的阻抗峰频率的变化。为了能够从噪音信号中将黄曲霉毒素 B1 的信号提取出来，采用了 K 均值聚类分析方法，实现了对该毒素的亚飞摩尔的检测，其检测限达到了 0.1 fg/mL [21]。如图 2 所示，该方法也被应用到有机电化场效应管(OECT)上来实时监控上皮组织的培养[22]，通过给 OECT 的门电位施加一定的均匀白噪音扰动，获取门控区域和驱动区域的电流噪音，进而获得培养的上皮组织的阻抗变换，该方法将检测的时间分辨率提高到毫秒级。

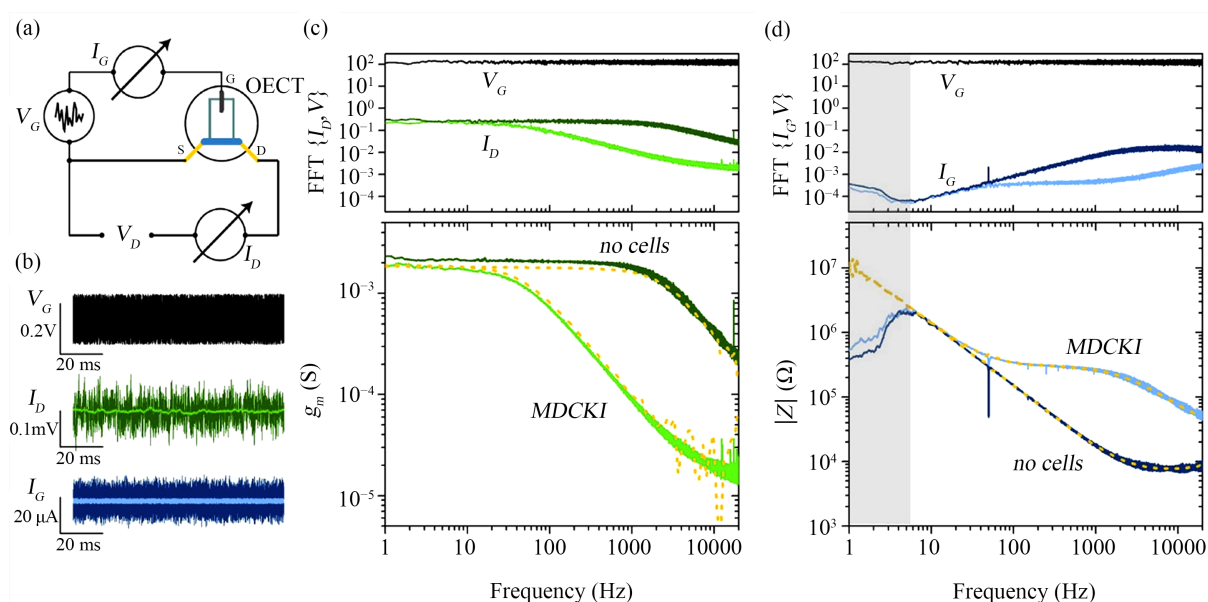


Figure 2. Noise-based impedance sensing with OECTs. (a) Wiring diagram of an OECT for noise based sensing. $V_D = -0.6$ V, applied V_G is uniform white noise of amplitude 100 mV, I_G and I_D can be measured individually or simultaneously. (b) Raw noise recording of applied white noise, V_G (black), as well as the measured current noise (I_D , green; I_G , blue) with cells (light colors) and without (dark colors). The FFT of 2 min noise recordings for the I_D based measurements (c) yielding the transconductance vs. frequency response of the ionic circuit, and of the I_G based measurements (d), providing an estimate of the system impedance. Dotted yellow lines are measurements of the same systems through a harmonic frequency sweeping approach. The grey region in (d) is dominated by ambient current noise, rendering data in this region useless for impedance sensing using the gate current. Reprinted with permission from ref. [22]. Copyright 2015 Springer

图 2. 基于有机电化场效应管(OECT)的阻抗噪音谱检测[22]。(a) 检测装置的示意图， $V_D = -0.6$ V， V_G 施加变化幅度为 100 mV 的均匀分布的白噪音信号， I_G 和 I_D 分别单独或同时测量。(b) 施加了白噪音后，原始噪音信号的记录。 V_G (黑色)，有细胞(浅色)和没有细胞状态下(深色)的电流扰动(I_D ，绿色； I_G ，蓝色)，记录时间 2 min。(c) 产生的转移电导和频率之间的响应。(d) 系统阻抗的估计，黄色点线是通过谐波频率扫描的方法对相同系统测出的阻抗值，图中灰色区域是受环境电流噪音控制，导致这个区域的数据在阻抗检测中无法使用

尽管阻抗检测方法的灵敏度很高,但也有一定的局限性。受制于电极表面双电层厚度的影响,当电极的检测距离超过双电层厚度时,电极界面电荷将被溶液中其他离子屏蔽掉,使检测的灵敏度下降。而生物样品的离子强度较高,而高离子强度溶液导致更小的双电层厚度,最终导致其无法适用于生物样品的检测。为解决双电层对电化学检测的影响,通过施加高频率的交流扰动,使电极表面无法形成双电层屏蔽效应来提高电极检测的距离。在理论上是可行的,但是存在着技术上的挑战[23],其关键因素主要在于电极的加工以及杂散电容对高频信号的影响。例如, Widdershoven [24]等人利用 CMOS 阵列纳米电容器件实现了对生物样品的高频交流阻抗的检测与细胞和粒子的实时成像[25],成功摆脱了双电层对电化学检测的影响,将电化学检测拓展到了高离子强度环境的生物样品实时检测上。

3.2. 场效应管

频域信号解析也被应用到了纳米线场效应管(nano wire field effect transistors, NWFET)的检测中。基于生物分子与功能化的纳米线结合之后介电性质的变化来实现检测的 NWFET 对界面状态的扰动极为敏感。尤其在低浓度体系中的检测很难判断这种信号是否是检测物质的信号。为解决这一问题, Lieber 等[26]通过对 NWFET 的时域信号进行功率谱密度分析将时域信号转为频域信号后,发现该检测器对前列腺特异性抗原(PSA)的检测灵敏度提高了 10 倍,检测限达到 0.15 pM,如图 3 所示。由于信号频域转换之后,抗原和抗体的结合信息隐藏在 $1/f$ 噪音谱中,通过将生物分子在 NWFET 表面结合关系的 Lorentzian 函数引入分析中,成功从频域噪音谱中解析出 PSA 与纳米线相互作用产生的信号。该项工作为提高场效应管单分子检测方法灵敏度和检测能力开拓一个新的途径[27] [28]。单分子在碳纳米管场效应管表面吸附过程中,因电荷扰动会产生相应的噪音。Akai-Kasaya 等[27]对该噪音谱进行了分析,从理论和实验上证明了基于场效应管检测的噪音分析,能够为单分子吸附过程提供分子与场效应管电子耦合强度和吸附分子带电状态等信息。这种通过对检测中的时域信号进行频域分析,获取生物分子检测中的相关动力学信息的方法被逐渐应用到其他的电化学检测方法中。

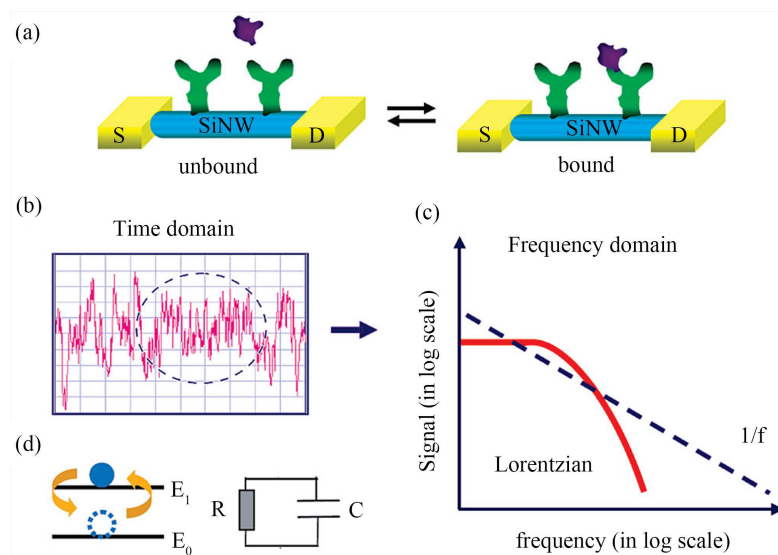


Figure 3. (a) Schematic of protein binding and unbinding to an antibody-modified SiNW FET sensor. S and D correspond to the source and drain metal contacts to the NW. (b) A schematic of electrical noise in a time-domain measurement. (c) Schematic of Lorentzian and $1/f$ functions in the frequency domain. (d) Models of a two-level system (left) and a RC circuit (right). Reprinted with permission from ref. [26]. Copyright 2010 American Chemistry Society

图 3. (a) 蛋白质在抗体修饰的硅纳米线场效应管传感器表面结合和解离的示意图。S 和 D 分别是纳米线的源极和驱动极。(b) 时域体系测量的电流噪音。(c) 频域体系中的洛伦茨和 $1/f$ 噪音曲线。(d) 两水平系统模型(左)和等效电路(右) [26]

3.3. 电化学氧化还原循环放大

如上所述,通过对电化学检测中的信号进行统计和频域处理,也可以从中获取电化学过程中隐藏的一些信息。Lemay 等[29] [30] [31]通过对电化学检测中电流噪音的分析,创立电化学相关谱的技术。通过构建带有两电极的纳米薄层电解池,研究二茂铁二甲醇在两电极之间的氧化还原循环反应的电流扰动信息[30]。由于两电极在纳米薄层池中,物质在纳米尺度下扩散速度较快,产生类似于荧光相关光谱的电流扰动信号。通过对该扰动信号进行时间相关分析,最终获取二茂铁二甲醇在电极表面的吸附动力学信息。依据高频段信号,还可推测二茂铁二甲醇的吸附和解吸速率。利用该方法可实现在纳流控装置中超低体积流动的测定[29],单分子测量[31]。

通过对电化学扰动的的时间进行相关分析,可以获得扰动信号变化的频率。Lemay 等人通过 3D 随机漫步模拟和实验验证,分析了纳米尺寸薄层池中因电活性物质浓度变化对电化学氧化还原循环反应的信号产生扰动的噪音特征[32]。通过对扰动信号幅值变化大小的分析,能够获取电化学活性物质参与反应或者界面吸附过程的平衡态信息[33],如图 4 所示。尽管这些开创性的研究工作已经证明了利用电化学方法来监控单分子行为的可行性,但是将其应用到实际样品还必须进一步提升扰动信号(时序信号)获取与分析方法,获取隐藏在信号扰动中的可靠信息(如检测神经元胞吐等)。

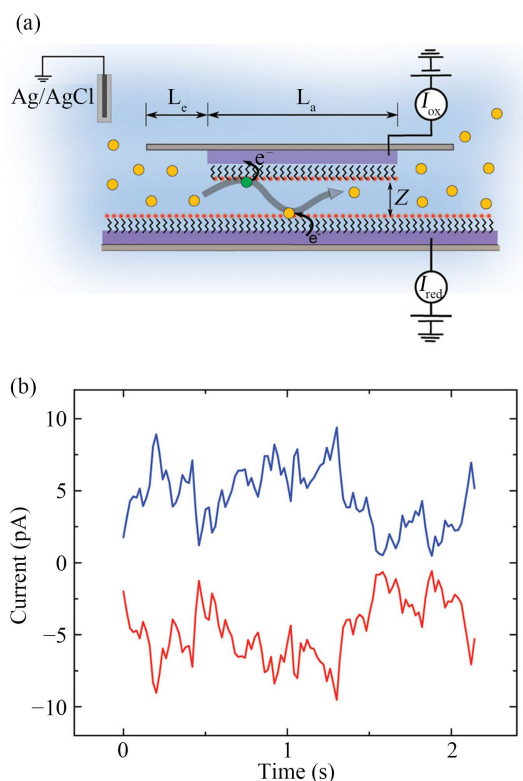


Figure 4. (a) Schematic of a nanofluidic thin-layer cell with two independently addressable electrodes functionalized with SAMs and separated by a nanometer scale distance, z . L_c is the length of the access nanochannel leading to the active region while the active region has a length L_a . (b) Fluctuations in the amperometric traces obtained for $100 \mu\text{M}$ $\text{Fc}(\text{MeOH})_2$. The DC component has been offset to focus on the fluctuations. The amplitudes of the traces for the oxidizing (blue) and reducing (red) electrodes are directly correlated, but the currents are opposite in sign as expected for redox cycling. Reprinted with permission from ref. [33]. Copyright 2011 American Chemistry Society

图 4. (a) 纳流控薄层池示意图,薄层池上下两端为单分子层自主装的功能化电极,两个电极之间的距离为纳米尺度(z), L_c 为进入薄层池检测区域的通道长度, L_a 是薄层池检测区域的长度。(b) $100 \mu\text{M}$ 的二茂铁二甲醇在纳流控薄层池中产生的电流扰动,氧化电流(蓝色)和还原电流(红色)之间直接相关,电流数值的符号相反[33]

3.4. 纳米孔电化学检测

基于纳米孔的电化学分析是目前在单分子检测上发展较快的领域，在粒子检测、DNA 分析与蛋白质检测上得到了广泛的应用。在处理单分子物质穿过纳米孔的实验数据的过程中，逐步发展出来的一些方法为扰动信号分析提供了有益的借鉴。首先，为了将纳米孔本身的噪音与物质穿过纳米孔的噪音分辨开，一系列的早期研究将关注点放在纳米孔自身的电化学噪音上。Golovchenko 等[34]研究了固态氮化硅纳米孔表面电荷的扰动对离子穿孔电流噪音的影响，探讨了如何选择合适的 pH 来减小通过纳米孔的离子电流扰动，如图 5 所示。Siwy 等[35]研究了处于整流状态下的聚合物纳米孔(PET)，玻璃纳米孔，氮化硅纳米孔的 $1/f$ 噪音。发现了因纳米孔表面结构和电场分布的差异导致 PET 和玻璃纳米孔在高电导状态时离子电流的 $1/f$ 噪音扰动呈现非平衡态的性质；揭示了离子与纳米通道表面相互作用对 $1/f$ 噪音的影响，为降低纳米通道电流测量的低频噪音提供解决途径。而在 1993 和 1994 年已经有文献报道将电流噪音的扰动应用到蛋白质纳米孔的氨基酸基团质子化[36]以及糖基结合动力学[37]分析。利用该分析方法，Bezrukov 等通过功率谱密度分析了氨苄西林与外膜蛋白 G 通道结合引起的噪音扰动，并对结合过程进行了动力学分析[38]。通过纳米通道离子电流的白噪音分析，揭示了通道的传输机制随着离子浓度而发生变化。在低盐浓度，生物纳米通道中表面电荷控制离子传输；在高盐浓度下，盐溶液的吸附过程控制离子传输[39]。为了进一步拓展纳米孔中离子噪音分析，提高纳米孔电化学检测灵敏度，一系列关于纳米孔离子电流噪音的产生机制的研究得到了报道。Bonthuis 等通过理论模拟，分析了离子通过纳米孔的电流噪音，发现随着离子浓度增加，离子之间相互作用导致低频下幂律型分布的噪音谱[40]，而纳米通道中流体流动对纳米孔离子电流信号的噪音谱的形状则没有影响[41]。Deeker 等建立了数学模型来考虑纳米孔表面和纳米孔接触区域对离子电流噪音的贡献[42]；Bocquet 等利用理论分析证明了离子在纳米孔表面吸附过程直接导致了低频下 $1/f$ 噪音[43]；Rigo 等通过离子通过亚纳米孔的离子噪音谱分析，发现离子噪音谱与电流关系存在这一个临界值，低于临界值的噪音谱密度与电流无关，而高于临界值的噪音谱密度随着电流值成二次曲线的关系，通过实验和理论分析，揭示了亚纳米通道电流噪音功率谱密度和离子的溶剂化层扭曲的程度有关[44]。随着离子种类的不同，离子电流噪音谱密度的临界值也在变化，说明通过离子电流扰动分析，确实能够发现信号扰动背后隐藏的信息。

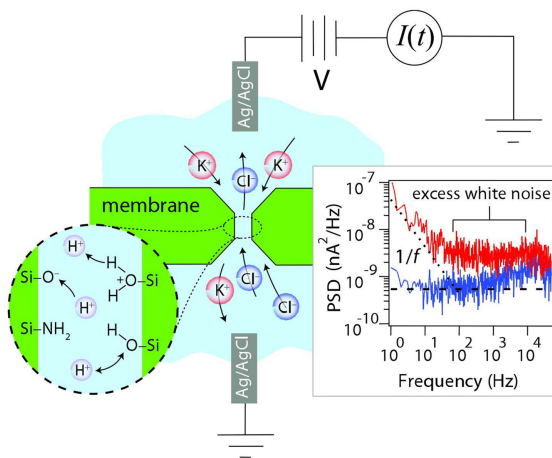


Figure 5. A nanopore is a narrow channel in a thin Si₃N₄ membrane. A current of electrolyte ions flows through the nanopore in response to an applied voltage. Detail: surface protonization reactions. Inset: Typical current noise spectra at 0 mV (lower trace) and 150 mV (upper trace) applied voltage at 1 M KCl and neutral pH. Reprinted with permission from ref. [34]. Copyright 2009 American Physical Society

图 5. 氮化硅纳米孔，离子在电压的驱动下通过纳米孔产生电流[34]。纳米孔放大区域图是纳米孔内表面质子化反应过程。内插图：典型电流噪音谱，驱动电压在 0 V 和 150 mV，溶液为 1 M KCl，pH 为中性

3.5. 基于纳米孔离子电流信号扰动的信息提取

纳米孔的体积与单个 DNA、单个蛋白质分子以及单个纳米粒子的体积相当。当这些分子或粒子通过纳米孔时，纳米孔的电阻发生变化进而产生过孔离子电流的扰动。在利用一定的方法修饰纳米孔，控制生物分子以及纳米粒子与纳米孔的相互作用以减少该作用导致的噪音下，产生电流扰动变化的幅度则是与过孔分子或粒子的尺寸和形状有关；电流扰动变化的频率(扰动持续的时间)与过孔分子或粒子的自身电荷相关[45]-[52]。Mayer 课题组在前期工作的基础上[45]，通过理论和实验相结合的方法[53]，对过孔分子引起的离子电流扰动进行了分析，一次性获取了单个蛋白质分子的五个特性参数[46] [53] (形状、体积、电荷、转动扩散系数和偶极矩)。如果采用合适的捕获技术，控制同一分子或粒子往复的穿过纳米孔，可增加过孔电流扰动，进而提高获取分子或粒子特性参数的精度。例如，通过压力与电压共同控制纳米粒子传输过程，实现对纳米粒子尺寸的亚纳米精度的测量[54]。

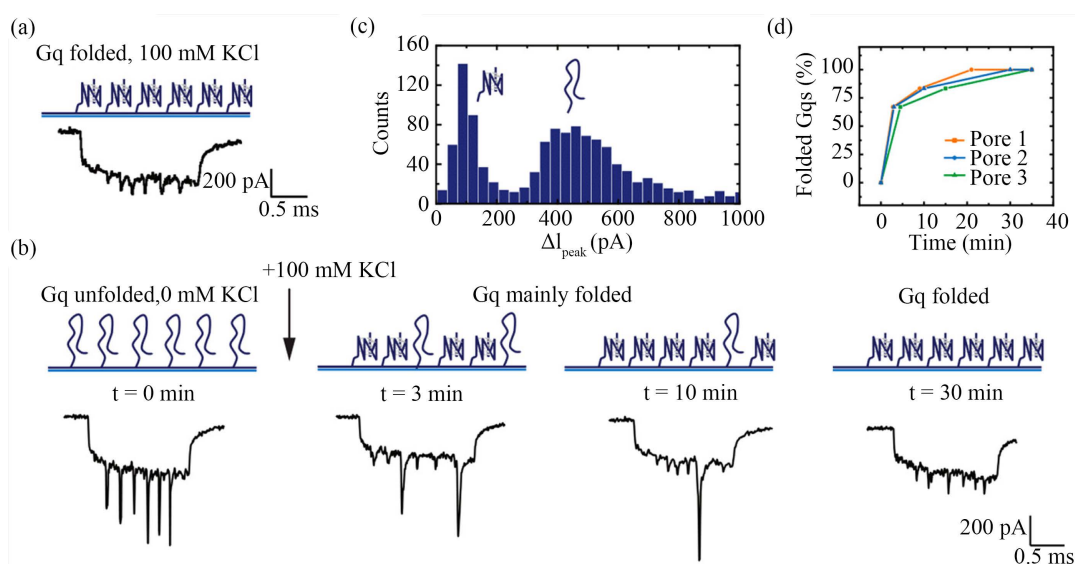


Figure 6. smDNA discriminates unfolded and folded Gq. Each peak represents one T30695 Gq attached to DNA carrier. (a) Gq prefolded in 100 mM potassium chloride (KCl) in a nanopore measurement shows only folded Gqs. (b) Unfolded Gq in the absence of KCl induces deep peaks at the beginning of the measurement indicate unfolded Gq. Upon addition of unfolded Gqs in measurement buffer with 100 mM KCl, Gqs start to fold. In the first 3 min of measurement, the clear majority of Gqs are folded. Nanopores detect unfolded Gq even after 10 min. A period of 30 min is required for folding of all Gqs. (c) A clear difference between folded and unfolded Gqs from the current drop of peaks (ΔI_{peak}) can be observed. The lower ΔI_{peak} is attributed to folded Gqs, and higher current drop is coming from unfolded Gq. (d) Single-molecule kinetics of Gq folding for different nanopores is presented. Reprinted with permission from ref. [55]. Copyright 2019 American Chemistry Society

图 6. smDNA 区分 G-四聚体的折叠与展开，每一个峰代表一个 G-四聚体 T30695 附着 DNA 载体上[55]。(a) 纳米孔测定 100 mM KCl 溶液中 G-四聚体显示只有折叠状态的 G-四聚体。(b) G-四聚体在没有 KCl 存在时只显示更大的非折叠峰，当加入 100 mM KCl 时，G-四聚体开始折叠。在初始的 3 分钟内，大部分 G-四聚体折叠了，10 分钟后还有部分 G-四聚体没有折叠，30 分钟后，所有的 G-四聚体完全折叠了。(c) 折叠和未折叠的 G-四聚体的峰电流下降值具有明显差异，低的峰电流下降值代表折叠的 G-四聚体，高的峰电流下降值代表未折叠的 G-四聚体。(d) 不同尺寸的纳米孔测定的 G-四聚体折叠动力学过程

蛋白质和 DNA 等生物分子的构象对生物分子的功能具有重要作用，了解生物分子构象变化有助于掌握生物分子实现特定功能的必要途径。传统的分析技术，如圆二色谱、XRD、红外和质谱都需要对样品进行相关处理，难以在原位实时获取生物分子构象信息。荧光标记方法虽然能够获得实时信号，但是需要借助其他分析手段才能确定其构象类型。而利用纳米孔离子电流扰动研究捕获的生物分子构象变化则可以实现实时的观测，且无需对样品进行预处理。如图 6 所示，Keyser 课题组[55]利用离子电流信号扰

动分析技术, 成功地将 DNA G-四聚体向二聚体的转变与电流信号扰动相关联。Chen 等[56]采用 ClyA 生物纳米孔将单麦芽糖结合蛋白捕获在 ClyA 纳米孔内, 观察到还原糖与该蛋白质结合后的三种构象变化。Long 课题组[57]分析了 Poly(dA)₄ 与溶血素纳米孔之间弱相互作用产生离子电流扰动的频率谱变化, 揭示了它们之间相互作用的大小, 进而提出单分子离子谱的概念。

4. 光学方法

光学方法在单分子检测中已经达到较为广泛的应用, 例如单分子酶催化、聚合物的构象变化等。但是, 光学检测方法通常需要考虑其时间和空间分辨率的平衡, 也即是在提高时间分辨率时必然要牺牲其空间分辨率, 反之亦然。例如, 表面等离子共振和干涉显微镜技术在纳米粒子电荷成像中, 由于小尺寸纳米粒子的布朗运动导致这些方法很难在获得具有较高时间分辨率的成像结果。如图 7 所示, 为解决粒子布朗运动的问题, Tao 课题组采用聚合物将纳米粒子固定在界面上, 通过施加交变电场来获取纳米粒子因自身电荷或者与其它分子结合之后产生的扰动, 再通过快速傅里叶变换从扰动信息中获取纳米粒子的表面电荷[58]或者结合动力学过程[59]。该课题组还在前期工作基础之上, 通过测量单个分子结合反应之后的本身的热扰动不同, 获得了单分子结合能和自由能分布[60]。另外, 将纳米粒子的散射光与粒子极化动力学扰动结合起来, 建立了单粒子动态光散射技术[61], 实现了对不同形状粒子测量。总之, 通过分子或粒子自身性质变化产生的扰动, 可获取一定的物质本身及其相互作用的参数。利用可控扰动可规避单分子光学分析方法在空间与时间分辨上的困境。

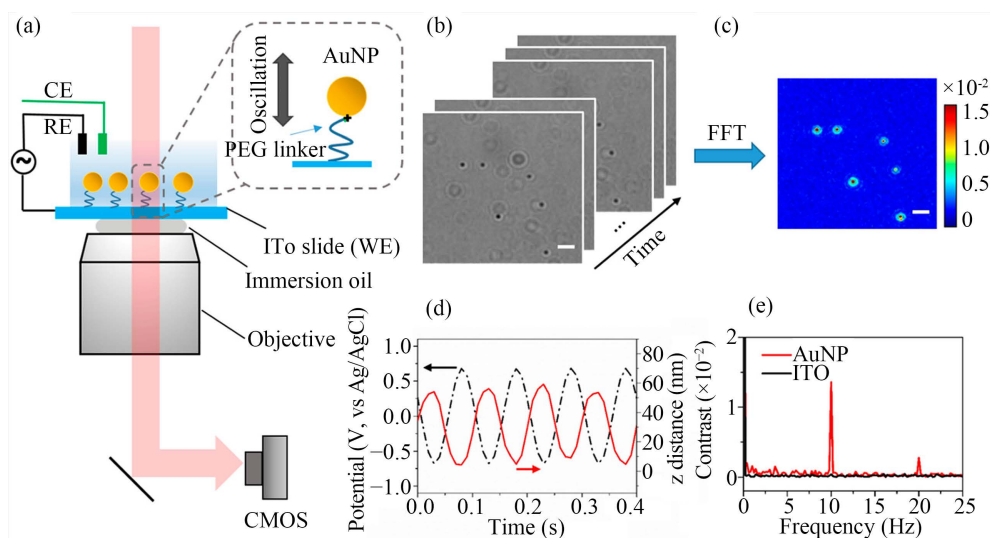


Figure 7. Imaging nanoparticles and charges with a bright field optical microscope. (a) Schematic illustration of the experimental setup, showing an AuNP tethered to an ITO slide surface with a polymer. The AuNP is driven into oscillation with an alternating electric field generated using a three-electrode electrochemical configuration, where WE, CE, and RE are working (ITO slide), counter (Pt coil), and reference (Ag/AgCl) electrodes, respectively. (b) Time sequence of bright field optical images of AuNPs recorded by a camera. (c) FFT image obtained by performing FFT on each pixel of the optical images in time domain. (d) Image contrast (converted to oscillation amplitude, red line) of an AuNP and applied potential (black line) vs time showing oscillation of the AuNP. (e) FFT spectra of the AuNP (red line) and ITO background (black line). Diameter of AuNP: 100 nm. Applied potential amplitude = 0.7 V, frequency = 10 Hz. Image scale bars in (b) and (c): 2 μm . Reprinted with permission from ref. [58]. Copyright 2019 American Chemistry Society

图 7. 明场光学显微镜测量纳米粒子及其电荷[58]。(a) 实验步骤示意图, 金纳米粒子通过聚合物修饰在 ITO 玻璃上, 金纳米粒子在交变电场驱动发生振荡。WE, CE, 和 RE 分别是工作电极、对电极和参比电极。(b) 明场显微镜获得的金纳米粒子振荡的时间序列图。(c) 对每一张时域的光学图进行傅里叶变换得到傅里叶变换图。(d) 金纳米粒子产生的振荡(红线)和施加电压变化(黑线)的对比图。(e) 金纳米粒子的傅里叶光谱(红线)和 ITO 的背景光谱(黑线), 金纳米粒子尺寸 100 nm, 施加电压幅度 0.7 V, 频率 10 Hz, (b)和(c)图的标尺是 2 μm

5. 数据分析方法

在机器学习算法得到广泛应用之前,对于扰动数据的分析大都依赖于快速傅里叶变换[62]、微分校准[63]等方法来抑制无关信号噪音。例如,在单个纳米粒子电化学反应瞬态测量过程中采用快速傅里叶变换和选择合适数字滤波对实验数据进行处理,可以极大地保留电流信号中所需的相关信号[62]。然而,这些方法只适合处理单一样品数据,无法区分出混合样品产生的信号。为解决这一问题,研究者采用了频域分析的方法,将纳米粒子穿孔的时域电流信号转化为频域的相角值,再利用相角值变化区分出了混合纳米粒子溶液二氧化硅、银和金纳米粒子的信号[64]。然而,信号的相关滤波处理仍然依靠人的经验来设定,这就制约了这种方法在非专业人士中的推广。而机器学习算法强大的自我学习功能,可以通过一定量的数据的训练来自我判定信号处理的滤波频率以及噪音水平,为自动、高效、准确的处理数据提供了手段,特别在一些超高灵敏检测中得到了应用。Kim 课题组[65]采用深度学习算法将低于仪器检测限 H_2 信号提取出来,提升了仪器的检测能力。深度学习算法在 DNA [66]、蛋白质和病毒[67] [68] [69]检测的实验数据处理上也显现出强大的优势,能够自动确定电流信号的噪音水平和滤波频率,并且能够将电流阻断信号几乎相同的只有一个碱基差异的 DNA 分子识别出来[65],为纳米通道在实际的临床检测中应用提供了解决办法。

6. 信号扰动分析面临的挑战和发展方向

仪器和信息技术的发展使基于信号扰动的分析检测技术能够得以实现,但是一些实际问题仍然有待解决。首先,任何基于信号扰动的分析技术都需要将不可控的信号扰动降到最低,避免产生错误的分析结果;其次,提升检测方法的重现性以及在实际应用中的可靠性;最后,对于基于机器学习算法的检测方法需要建立大量可靠的基于不同样品的信号数据库,提高算法在应用过程中准确性。这些挑战是信号扰动分析技术发展中必须克服,也为该方法的发展指出方向,最终能够脱离实验室的研究,发展成为在实际应用中可靠、灵敏、快速的检测方法。

7. 背景噪音的抑制与解决办法

综上所述,当分析方法的检测灵敏度接近亚皮摩尔以下时,被检测物的响应信号相对较弱,以致于经常被掩盖在背景噪音中。由于背景噪音来源复杂,很难被消除,因此,必须采用一定的方法来抑制背景噪音。首先,分析噪音的来源和其在不同频率上的分布是确定哪一种噪音是主要影响因素的关键。例如,热噪音主要分布在低频范围[70],如果检测方法的时间分辨率较低,那么就需要考虑热运动对背景噪音的贡献,采用降低热运动的方式抑制热噪音。其次,对于环境噪音可以采用物理屏蔽的方法来隔离和抑制它。而检测仪器自身的噪音的无法避免,需要通过数学处理方法将检测信号与检测仪器自身的信号扰动分离出来。因为仪器自身的信号扰动是在一个固有的频率范围内,通过频域分析可以将该噪音信号分离出去,进而提取出被检测物的信号。

8. 结论

综上所述,信号扰动分析为超高灵敏度的检测提供一种方案,它将被检测物的自身扰动作为一种信号源,其直接反映了被检测物自身性质的变化。但是,该信息通常被背景噪音信号所掩盖,需要通过一定的方法将其提取出来。由于被检测物自身的特异性导致其产生的信号扰动区分度较大,因而能够实现超高灵敏度的检测。信号的获取和处理,依赖于仪器以及数学工具的运用;随着技术的发展,该方法终将能够在复杂样品中痕量物质的检测。

致 谢

感谢国家自然科学基金面上项目(21974058, 21775066)资助。感谢南通大学高层次人才科研启动经费的资助。

基金项目

国家自然科学基金面上项目(21974058, 21775066)资助。

参考文献

- [1] Gubala, V., Harris, L.F., Ricco, A.J., Tan, M.X. and Williams, D.E. (2011) Point of Care Diagnostics: Status and Future. *Analytical Chemistry*, **84**, 487-515. <https://doi.org/10.1021/ac2030199>
- [2] Kelley, S.O. (2016) What Are Clinically Relevant Levels of Cellular and Biomolecular Analytes? *ACS Sensors*, **2**, 193-197. <https://doi.org/10.1021/acssensors.6b00691>
- [3] Wu, Y.F., Tilley, R.D. and Gooding, J.J. (2018) Challenges and Solutions in Developing Ultrasensitive Biosensors. *Journal of the American Chemical Society*, **141**, 1162-1170. <https://doi.org/10.1021/jacs.8b09397>
- [4] Singh, P.S. and Lemay, S.G. (2016) Stochastic Processes in Electrochemistry. *Analytical Chemistry*, **88**, 5017-5027. <https://doi.org/10.1021/acs.analchem.6b00683>
- [5] Bizzarri, A.R. and Cannistraro, S. (2013) $1/f(\alpha)$ Noise in the Dynamic Force Spectroscopy Curves Signals the Occurrence of Biorecognition. *Physical Review Letters*, **110**, Article ID: 048104. <https://doi.org/10.1103/PhysRevLett.110.048104>
- [6] Bizzarri, A.R. and Cannistraro, S. (2014) Antigen-Antibody Biorecognition Events as Discriminated by Noise Analysis of Force Spectroscopy Curves. *Nanotechnology*, **25**, Article ID: 335102. <https://doi.org/10.1088/0957-4484/25/33/335102>
- [7] Bizzarri, A.R. (2016) Energy Landscape Investigation by Wavelet Transform Analysis of Atomic Force Spectroscopy Data in a Biorecognition Experiment. *Journal of Biological Physics*, **42**, 167-176. <https://doi.org/10.1007/s10867-015-9398-8>
- [8] Bizzarri, A.R., Vegh, A.G., Varo, G. and Cannistraro, S. (2019) Interaction Force Fluctuations in Antigen-Antibody Biorecognition Studied by Atomic Force Spectroscopy. *ACS Omega*, **4**, 3627-3634. <https://doi.org/10.1021/acsomega.8b02993>
- [9] Kasas, S., Malovichko, A., Villalba, M.I., Vela, M.E., Yantorno, O. and Willaert, R.G. (2021) Nanomotion Detection-Based Rapid Antibiotic Susceptibility Testing. *Antibiotics*, **10**, Article No. 287. <https://doi.org/10.3390/antibiotics10030287>
- [10] Kasas, S., Ruggeri, F.S., Benadiba, C., Maillard, C., Stupar, P., Tournu, H., Dietler, G. and Longo, G. (2015) Detecting Nanoscale Vibrations as Signature of Life. *Proceedings of the National Academy of Sciences of the United States of America*, **112**, 378-381. <https://doi.org/10.1073/pnas.1415348112>
- [11] Willaert, R.G., Vanden Boer, P., Malovichko, A., Alioscha-Perez, M., Radotic, K., Bartolic, D., Kalauzi, A., Villalba, M.I., Sanglard, D., Dietler, G., Sahli, H. and Kasas, S. (2020) Single Yeast Cell Nanomotions Correlate with Cellular Activity. *Science Advances*, **6**, 1-8. <https://doi.org/10.1126/sciadv.aba3139>
- [12] Shabi, O., Natan, S., Kolel, A., Mukherjee, A., Tchaicheeyan, O., Wolfenson, H., Kiryati, N. and Lesman, A. (2020) Motion Magnification Analysis of Microscopy Videos of Biological Cells. *PLoS ONE*, **15**, Article ID: e0240127. <https://doi.org/10.1371/journal.pone.0240127>
- [13] Kwon, T., Gunasekaran, S. and Eom, K. (2019) Atomic Force Microscopy-Based Cancer Diagnosis by Detecting Cancer-specific Biomolecules and Cells. *Biochimica et Biophysica Acta—Reviews on Cancer*, **1871**, 367-378. <https://doi.org/10.1016/j.bbcan.2019.03.002>
- [14] Ruggeri, F.S., Sneideris, T., Vendruscolo, M. and Knowles, T.P.J. (2019) Atomic Force Microscopy for Single Molecule Characterisation of Protein Aggregation. *Archives of Biochemistry and Biophysics*, **664**, 134-148. <https://doi.org/10.1016/j.abb.2019.02.001>
- [15] Valotteau, C., Sumbul, F. and Rico, F. (2019) High-Speed Force Spectroscopy: Microsecond Force Measurements Using Ultrashort Cantilevers. *Biophysical Reviews*, **11**, 689-699. <https://doi.org/10.1007/s12551-019-00585-4>
- [16] Lissandrello, C., Inci, F., Francom, M., Paul, M.R., Demirci, U. and Ekinici, K.L. (2014) Nanomechanical Motion of *Escherichia coli* Adhered to a Surface. *Applied Physics Letters*, **105**, Article ID: 113701. <https://doi.org/10.1063/1.4895132>

- [17] Yu, H., Siewny, M.G.W., Edwards, D.T., Sanders, A.W. and Perkins, T.T. (2017) Hidden Dynamics in the Unfolding of Individual Bacteriorhodopsin Proteins. *Science*, **355**, 945-950. <https://doi.org/10.1126/science.aah7124>
- [18] Beaussart, A. and El-Kirat-Chatel, S. (2019) Microbial Adhesion and Ultrastructure from the Single-Molecule to the Single-Cell Levels by Atomic Force Microscopy. *The Cell Surface*, **5**, Article ID: 100031. <https://doi.org/10.1016/j.tcsw.2019.100031>
- [19] Newton, R., Delguste, M., Koehler, M., Dumitru, A.C., Laskowski, P.R., Mueller, D.J. and Alsteens, D. (2017) Combining Confocal and Atomic Force Microscopy to Quantify Single-Virus Binding to Mammalian Cell Surfaces. *Nature Protocols*, **12**, 2275-2292. <https://doi.org/10.1038/nprot.2017.112>
- [20] Ghosh, H. and Roy Chaudhuri, C. (2013) Ultrasensitive Food Toxin Biosensor Using Frequency Based Signals of Silicon Oxide Nanoporous Structure. *Applied Physics Letters*, **102**, Article ID: 243701. <https://doi.org/10.1063/1.4811409>
- [21] Ghosh, H. and Roy Chaudhuri, C. (2015) Noise Spectroscopy as An Efficient Tool for Impedance Based Sub-Femtomolar Toxin Detection in Complex Mixture Using Nanoporous Silicon Oxide. *Biosensors and Bioelectronics*, **67**, 757-762. <https://doi.org/10.1016/j.bios.2014.09.035>
- [22] Rivnay, J., Leleux, P., Hama, A., Ramuz, M., Huerta, M., Malliaras, G.G. and Owens, R.M. (2015) Using White Noise to Gate Organic Transistors for Dynamic Monitoring of Cultured Cell Layers. *Scientific Reports*, **5**, Article ID: 11613. <https://doi.org/10.1038/srep11613>
- [23] Kulkarni, G.S. and Zhong, Z. (2012) Detection Beyond the Debye Screening Length in a High-Frequency Nanoelectronic Biosensor. *Nano Letters*, **12**, 719-723. <https://doi.org/10.1021/nl203666a>
- [24] Laborde, C., Pittino, F., Verhoeven, H.A., Lemay, S.G., Selmi, L., Jongsma, M.A. and Widdershoven, F.P. (2015) Real-Time Imaging of Microparticles and Living Cells with CMOS Nanocapacitor Arrays. *Nature Nanotechnology*, **10**, 791-795. <https://doi.org/10.1038/nnano.2015.163>
- [25] Cossetini, A., Laborde, C., Brandalise, D., Widdershoven, F., Lemay, S.G. and Selmi, L. (2021) Space and Frequency Dependence of Nanocapacitor Array Sensors Response to Microparticles in Electrolyte. *IEEE Sensors Journal*, **21**, 4696-4704. <https://doi.org/10.1109/JSEN.2020.3032712>
- [26] Zheng, G., Gao, X.P.A. and Lieber, C.M. (2010) Frequency Domain Detection of Biomolecules Using Silicon Nanowire Biosensors. *Nano Letters*, **10**, 3179-3183. <https://doi.org/10.1021/nl1020975>
- [27] Setiadi, A., Fujii, H., Kasai, S., Yamashita, K.-I., Ogawa, T., Ikuta, T., Kanai, Y., Matsumoto, K., Kuwahara, Y. and Akai-Kasaya, M. (2017) Room-Temperature Discrete-Charge-Fluctuation Dynamics of a Single Molecule Adsorbed on a Carbon Nanotube. *Nanoscale*, **9**, Article ID: 10674-10683. <https://doi.org/10.1039/C7NR02534C>
- [28] Vasudevan, S. and Ghosh, A.W. (2014) Using Room Temperature Current Noise to Characterize Single Molecular Spectra. *ACS Nano*, **8**, 2111-2117. <https://doi.org/10.1021/nn404526w>
- [29] Mathwig, K., Mampallil, D., Kang, S. and Lemay, S.G. (2012) Electrical Cross-Correlation Spectroscopy: Measuring Picoliter-per-Minute Flows in Nanochannels. *Physical Review Letters*, **109**, Article ID: 118302. <https://doi.org/10.1103/PhysRevLett.109.118302>
- [30] Zevenbergen, M.A.G., Singh, P.S., Goluch, E.D., Wolfrum, B.L. and Lemay, S.G. (2009) Electrochemical Correlation Spectroscopy in Nanofluidic Cavities. *Analytical Chemistry*, **81**, 8203-8212. <https://doi.org/10.1021/ac9014885>
- [31] Zevenbergen, M.A.G., Singh, P.S., Goluch, E.D., Wolfrum, B.L. and Lemay, S.G. (2011) Stochastic Sensing of Single Molecules in a Nanofluidic Electrochemical Device. *Nano Letters*, **11**, 2881-2886. <https://doi.org/10.1021/nl2013423>
- [32] Kaetelhoeven, E., Krause, K.J., Singh, P.S., Lemay, S.G. and Wolfrum, B. (2013) Noise Characteristics of Nanoscaled Redox-Cycling Sensors: Investigations Based on Random Walks. *Journal of the American Chemical Society*, **135**, 8874-8881. <https://doi.org/10.1021/ja3121313>
- [33] Singh, P.S., Chan, H.-S.M., Kang, S. and Lemay, S.G. (2011) Stochastic Amperometric Fluctuations as a Probe for Dynamic Adsorption in Nanofluidic Electrochemical Systems. *Journal of the American Chemical Society*, **133**, Article ID: 18289-18295. <https://doi.org/10.1021/ja2067669>
- [34] Hoogerheide, D.P., Garaj, S. and Golovchenko, J.A. (2009) Probing Surface Charge Fluctuations with Solid-State Nanopores. *Physical Review Letters*, **102**, Article ID: 256804. <https://doi.org/10.1103/PhysRevLett.102.256804>
- [35] Powell, M.R., Sa, N., Davenport, M., Healy, K., Vassiouk, I., Letant, S.E., Baker, L.A. and Siwy, Z.S. (2011) Noise Properties of Rectifying Nanopores. *The Journal of Physical Chemistry C*, **115**, 8775-8783. <https://doi.org/10.1021/jp2016038>
- [36] Bezrukov, S.M. and Kasianowicz, J.J. (1993) Current Noise Reveals Protonation Kinetics and Number of Ionizable Sites in an Open Protein Ion Channel. *Physical Review Letters*, **70**, 2352-2355. <https://doi.org/10.1103/PhysRevLett.70.2352>
- [37] Nekolla, S., Andersen, C. and Benz, R. (1994) Noise Analysis of Ion Current through the Open and the Sugar-induced

- Closed State of the LamB Channel of Escherichia Coli Outer Membrane: Evaluation of the Sugar Binding Kinetics to the Channel Interior. *Biophysical Journal*, **66**, 1388-1397. [https://doi.org/10.1016/S0006-3495\(94\)80929-4](https://doi.org/10.1016/S0006-3495(94)80929-4)
- [38] Nestorovich, E.M., Danelon, C., Winterhalter, M. and Bezrukov, S.M. (2002) Designed to Penetrate: Time-resolved Interaction of Single Antibiotic Molecules with Bacterial Pores. *Proceedings of the National Academy of Sciences of the United States of America*, **99**, 9789-9794. <https://doi.org/10.1073/pnas.152206799>
- [39] Queral-Martín, M., Lidón López, M. and Alcaraz, A. (2015) Excess White Noise to Probe Transport Mechanisms in a Membrane Channel. *Physical Review E*, **91**, Article ID: 062704. <https://doi.org/10.1103/PhysRevE.91.062704>
- [40] Zorkot, M., Golestanian, R. and Bonthuis, D.J. (2016) The Power Spectrum of Ionic Nanopore Currents: The Role of Ion Correlations. *Nano Letters*, **16**, 2205-2212. <https://doi.org/10.1021/acs.nanolett.5b04372>
- [41] Zorkot, M., Golestanian, R. and Bonthuis, D.J. (2016) Current Fluctuations in Nanopores: The Effects of Electrostatic and Hydrodynamic Interactions. *The European Physical Journal Special Topics*, **225**, 1583-1594. <https://doi.org/10.1140/epjst/e2016-60152-y>
- [42] Fragasso, A., Pud, S. and Dekker, C. (2019) 1/f Noise in Solid-State Nanopores Is Governed by Access and Surface Regions. *Nanotechnology*, **30**, Article ID: 395202. <https://doi.org/10.1088/1361-6528/ab2d35>
- [43] Gravelle, S., Netz, R.R. and Bocquet, L. (2019) Adsorption Kinetics in Open Nanopores as a Source of Low-Frequency Noise. *Nano Letters*, **19**, 7265-7272. <https://doi.org/10.1021/acs.nanolett.9b02858>
- [44] Rigo, E., Dong, Z., Park, J.H., Kennedy, E., Hokmabadi, M., Almonte-Garcia, L., Ding, L., Aluru, N. and Timp, G. (2019) Measurements of the Size and Correlations Between Ions Using an Electrolytic Point Contact. *Nature Communications*, **10**, Article No. 2382. <https://doi.org/10.1038/s41467-019-10265-2>
- [45] Yusko, E.C., Johnson, J.M., Majd, S., Prangkio, P., Rollings, R.C., Li, J., Yang, J. and Mayer, M. (2011) Controlling Protein Translocation through Nanopores with Bio-Inspired Fluid Walls. *Nature Nanotechnology*, **6**, 253-260. <https://doi.org/10.1038/nnano.2011.12>
- [46] Yusko, E.C., Bruhn, B.R., Eggenberger, O.M., Houghtaling, J., Rollings, R.C., Walsh, N.C., Nandivada, S., Pindrus, M., Hall, A.R., Sept, D., Li, J., Kalonia, D.S. and Mayer, M. (2017) Real-Time Shape Approximation and Fingerprinting of Single Proteins Using a Nanopore. *Nature Nanotechnology*, **12**, 360-367. <https://doi.org/10.1038/nnano.2016.267>
- [47] Fologea, D., Ledden, B., McNabb, D.S. and Li, J. (2007) Electrical Characterization of Protein Molecules by a Solid-State Nanopore. *Applied Physics Letters*, **91**, Article ID: 053901. <https://doi.org/10.1063/1.2767206>
- [48] Robertson, J.W.F., Rodrigues, C.G., Stanford, V.M., Rubinson, K.A., Krasilnikov, O.V. and Kasianowicz, J.J. (2007) Single-Molecule Mass Spectrometry in Solution Using a Solitary Nanopore. *Proceedings of the National Academy of Sciences of the United States of America*, **104**, 8207-8211. <https://doi.org/10.1073/pnas.0611085104>
- [49] Raillon, C., Cousin, P., Traversi, F., Garcia-Cordero, E., Hernandez, N. and Radenovic, A. (2012) Nanopore Detection of Single Molecule RNAP-DNA Transcription Complex. *Nano Letters*, **12**, 1157-1164. <https://doi.org/10.1021/nl3002827>
- [50] Soni, G.V. and Dekker, C. (2012) Detection of Nucleosomal Substructures Using Solid-State Nanopores. *Nano Letters*, **12**, 3180-3186. <https://doi.org/10.1021/nl301163m>
- [51] Di Fiori, N., Squires, A., Bar, D., Gilboa, T., Moustakas, T.D. and Meller, A. (2013) Optoelectronic Control of Surface Charge and Translocation Dynamics in Solid-State Nanopores. *Nature Nanotechnology*, **8**, 946-951. <https://doi.org/10.1038/nnano.2013.221>
- [52] Yusko, E.C., Prangkio, P., Sept, D., Rollings, R.C., Li, J. and Mayer, M. Single-Particle Characterization of a Beta Oligomers in Solution. *ACS Nano*, **6**, 5909-5919. <https://doi.org/10.1021/nn300542q>
- [53] Houghtaling, J., Ying, C., Eggenberger, O.M., Fennouri, A., Nandivada, S., Acharjee, M., Li, J., Hall, A.R. and Mayer, M. (2019) Estimation of Shape, Volume, and Dipole Moment of Individual Proteins Freely Transiting a Synthetic Nanopore. *ACS Nano*, **13**, 5231-5242. <https://doi.org/10.1021/acs.nano.8b09555>
- [54] German, S.R., Hurd, T.S., White, H.S. and Mega, T.L. (2015) Sizing Individual Au Nanoparticles in Solution with Sub-Nanometer Resolution. *ACS Nano*, **9**, 7186-7194. <https://doi.org/10.1021/acs.nano.5b01963>
- [55] Boskovic, F., Zhu, J., Chen, K. and Keyser, U.F. (2019) Monitoring G-Quadruplex Formation with DNA Carriers and Solid-State Nanopores. *Nano Letters*, **19**, 7996-8001. <https://doi.org/10.1021/acs.nanolett.9b03184>
- [56] Li, X., Lee, K.H., Shorkey, S., Chen, J. and Chen, M. (2020) Different Anomeric Sugar Bound States of Maltose Binding Protein Resolved by a Cytolysin Nanopore Tweezer. *ACS Nano*, **14**, 1727-1737. <https://doi.org/10.1021/acs.nano.9b07385>
- [57] Liu, S.C., Li, M.X., Li, M.Y., Wang, Y.Q., Ying, Y.L., Wan, Y.J. and Long, Y.T. (2018) Measuring a Frequency Spectrum for Single-Molecule Interactions with a Confined Nanopore. *Faraday Discussions*, **210**, 87-99. <https://doi.org/10.1039/C8FD00023A>

- [58] Zhu, H., Ma, G., Wan, Z., Wang, H. and Tao, N. (2020) Detection of Molecules and Charges with a Bright Field Optical Microscope. *Analytical Chemistry*, **92**, 5904-5909. <https://doi.org/10.1021/acs.analchem.9b05750>
- [59] Ma, G., Shan, X., Wang, S. and Tao, N. (2019) Quantifying Ligand-Protein Binding Kinetics with Self-Assembled Nano-Oscillators. *Analytical Chemistry*, **91**, Article ID: 14149-14156. <https://doi.org/10.1021/acs.analchem.9b04195>
- [60] Wang, H., Tang, Z., Wang, Y., Ma, G. and Tao, N. (2019) Probing Single Molecule Binding and Free Energy Profile with Plasmonic Imaging of Nanoparticles. *Journal of the American Chemical Society*, **141**, Article ID: 16071-16078. <https://doi.org/10.1021/jacs.9b08405>
- [61] Guerra, L.F., Muir, T.W. and Yang, H. (2019) Single-Particle Dynamic Light Scattering: Shapes of Individual Nanoparticles. *Nano Letters*, **19**, 5530-5536. <https://doi.org/10.1021/acs.nanolett.9b02066>
- [62] Gutierrez-Portocarrero, S., Sauer, K., Karunathilake, N., Subedi, P. and Alpuche-Aviles, M.A. (2020) Digital Processing for Single Nanoparticle Electrochemical Transient Measurements. *Analytical Chemistry*, **92**, 8704-8714. <https://doi.org/10.1021/acs.analchem.9b05238>
- [63] Gu, Z., Ying, Y.L., Cao, C., He, P. and Long, Y.T. (2019) Accurate Data Process for Nanopore Analysis. *Analytical Chemistry*, **87**, 907-913. <https://doi.org/10.1021/ac5028758>
- [64] Liu, X., Zeng, Q., Liu, C. and Wang, L. (2020) A Fourier Transform-Induced Data Process for Label-Free Selective Nanopore Analysis Under Sinusoidal Voltage Excitations. *Analytical Chemistry*, **92**, Article ID: 11635-11643. <https://doi.org/10.1021/acs.analchem.0c01339>
- [65] Cho, S.Y., Lee, Y., Lee, S., Kang, H., Kim, J., Choi, J., Ryu, J., Joo, H., Jung, H.T. and Kim, J. (2020) Finding Hidden Signals in Chemical Sensors Using Deep Learning. *Analytical Chemistry*, **92**, 6529-6537. <https://doi.org/10.1021/acs.analchem.0c00137>
- [66] Wei, Z.X., Ying, Y.L., Li, M.Y., Yang, J., Zhou, J.L., Wang, H.F., Yang, B.Y. and Long, Y.T. (2019) Learning Shapelets for Improving Single-Molecule Nanopore Sensing. *Analytical Chemistry*, **91**, Article ID: 10033-10039. <https://doi.org/10.1021/acs.analchem.9b01896>
- [67] Arima, A., Harlisa, I.H., Yoshida, T., Tsutsui, M., Tanaka, M., Yokota, K., Tonomura, W., Yasuda, J., Taniguchi, M., Washio, T., Okochi, M. and Kawai, T. (2018) Identifying Single Viruses Using Biorecognition Solid-State Nanopores. *Journal of the American Chemical Society*, **140**, Article ID: 16834-16841. <https://doi.org/10.1021/jacs.8b10854>
- [68] Arima, A., Tsutsui, M., Harlisa, I.H., Yoshida, T., Tanaka, M., Yokota, K., Tonomura, W., Taniguchi, M., Okochi, M., Washio, T. and Kawai, T. (2018) Selective Detections of Single-viruses Using Solid-state Nanopores. *Scientific Reports*, **8**, Article No. 16305. <https://doi.org/10.1038/s41598-018-34665-4>
- [69] Arima, A., Tsutsui, M., Yoshida, T., Tatematsu, K., Yamazaki, T., Yokota, K., Kuroda, S.I., Washio, T., Baba, Y. and Kawai, T. (2020) Digital Pathology Platform for Respiratory Tract Infection Diagnosis via Multiplex Single-Particle Detections. *ACS Sensors*, **5**, 3398-3403. <https://doi.org/10.1021/acssensors.0c01564>
- [70] Alessio, F., Sonja, S. and Cees, D. (2020) Comparing Current Noise in Biological and Solid-State Nanopores. *ACS Nano*, **14**, 1338-1349. <https://doi.org/10.1021/acsnano.9b09353>